Standing on the Shoulders of Giants: Rethinking EEG Foundation Model Pretraining via Multi-Teacher Distillation

Anonymous Authors[1]

Abstract

Pretraining for electroencephalogram (EEG) foundation models has predominantly relied on self-supervised masked reconstruction, a paradigm largely adapted from and inspired by the success of vision and language foundation models. However, unlike images and text, EEG datasets are notoriously expensive to collect and characterized by low signal-to-noise ratio. These challenges introduce difficulties in scaling the EEG foundation models and capturing the underlying neural semantics through reconstruction. In this work, we ask the question: can we stand on the shoulders of well-established foundation models from well-represented modalities to bootstrap the pretraining of EEG foundation models? We first demonstrate that mainstream foundation models, such as those from vision and time series, transfer surprisingly well to EEG domain. To this end, we propose the Multi-Teacher Distillation Pretraining (MTDP) framework for pretraining EEG foundation models via a two-stage multi-teacher distillation. In the first stage, we introduce a learnable gating network to fuse representations from diverse teachers (e.g., DINOv3 and Chronos) via a masked latent denoising objective. In the second stage, we distill the fused representation into an EEG foundation model. Extensive evaluations across 9 downstream tasks and 12 datasets demonstrate that our MTDP-based EEG foundation model outperforms its self-supervised counterparts while requiring only 25% of the pretraining data.

1. Introduction

Electroencephalogram (EEG) signals record the spontaneous electrical activity of the brain through electrodes placed on the scalp (Siuly et al., 2017). It has become a fundamental tool for assisting clinical diagnosis, advancing neuroscience and cognitive science research, developing brain-computer interface (BCI), and is considered the gold standard for sleep staging (Berry et al., 2017) and epilepsy diagnosis (Fisher et al., 2017). Although EEG recordings have traditionally been analyzed by highly trained specialists, deep learning has not only succeeded in automating such analysis, but also in unlocking new applications for EEG where data were not traditionally read by humans. Deep learning models, such as convolutional neural networks and recurrent neural networks, have demonstrated exceptional performance across a variety of tasks: seizure detection (Alotaiby et al., 2014), sleep staging (Aboalayon et al., 2016), emotion recognition (Li et al., 2022b), and motor imagery classification (Altaheri et al., 2023). However, early EEG-based deep learning models are often tailored to specific tasks and datasets, with limited ability to generalize beyond strictly defined experimental setups.

Following the remarkable success of foundation models (FMs) in computer vision and natural language processing, there is growing interest in developing similar FMs for EEG. This presents a paradigm shift away from training task and dataset specific models, to learning universal neural representations for models that can be adapted to a wide range of downstream tasks (Yang et al., 2023; Zhang et al., 2023). In particular, the pretraining of existing EEG FMs predominantly relies on masked reconstruction, where the model learns to predict missing patches of the input signal. Subsequently, these pretrained models are fine-tuned with a classification head, demonstrating state-of-the-art performance across diverse benchmarks (Jiang et al., 2024; Wang et al., 2025; Ouahidi et al., 2025).

Unlike natural language or images, EEG data are significantly more challenging to collect and share due to strict privacy constraints. Consequently, existing EEG datasets remain orders of magnitude smaller than the internet-scale corpora used to train vision (Siméoni et al., 2025) and language (Grattafiori et al., 2024) FMs, thereby challenging the scaling of EEG FMs. Furthermore, EEG signals are characterized by an exceptionally low signal-to-noise ratio, by which reconstruction-based objectives inherently prioritize

[1]Anonymous Institution, Anonymous City, Anonymous Region, Anonymous Country. Correspondence to: Anonymous Author <anon.email@domain.com>.

Preliminary work. Under review by the International Conference on Machine Learning (ICML). Do not distribute.

the modelling of artifacts and noise, effectively directing the model away from meaningful neural dynamics. The scarcity of data and the sensitivity to noise call for more data-efficient representation learning strategies that leverage external priors, rather than rely solely on masked reconstruction. This naturally raises the question: can we stand on the shoulders of well-established FMs from well-represented modalities to bootstrap the pretraining of an EEG FM?

In this work, we start by showing that mainstream FMs are surprisingly good at extracting EEG representations through a series of linear probing experiments. We then propose the Multi-Teacher Distillation Pretraining (MTDP) framework to pretrain EEG FM via two-stage multi-teacher distillation. In the first stage, we introduce a learnable gating network to weigh the importance of each teacher model and fuse teacher representations in an unsupervised manner. The second stage pretrains EEG FM by learning from the fused teacher representations through distillation. Figure 1 provides a comparison of masked reconstruction pretraining used in existing EEG FMs and the proposed MTDP framework. Our contributions can be summarized as follows:

- We show that vision FM, DINOv3, despite being trained on a different modality, transfer surprisingly well to EEG tasks, outperforming specialized EEG FMs under the linear probing setting.
- We explore multi-teacher knowledge distillation from vision and time series FMs as a data-efficient alternative to large-scale self-supervised pretraining for EEG.
- To leverage the complementary representations from teacher FMs of different modalities, we present a learnable gating network to weigh each teacher via a masked latent denoising objective and fuse teacher representations in an unsupervised manner.
- We demonstrate that distilled EEG FM consistently surpasses state-of-the-art self-supervised counterparts, in both linear probing and full fine-tuning settings, while only requiring 25% of pretraining data.

2. Related Works

2.1. EEG Foundation Model

Deep learning models for automated EEG analysis have undergone a paradigm shift from task-specific supervised learning to FMs that are capable of achieving state-of-the-art results on a variety of downstream tasks. Early efforts demonstrated the viability of learning universal biosignal representations by aggregating diverse datasets for pretraining (Yang et al., 2023), followed by subsequent work that scaled the pretraining to larger datasets (Zhang et al., 2023; Yuan et al., 2024; Jiang et al., 2024). The pretraining strategy for EEG FMs focuses on self-supervised learning, specifically masked reconstruction, aiming to reconstruct masked segments in the temporal domain (Yang et al., 2023; Chen et al., 2024; Wang et al., 2025), frequency domain (Jiang et al., 2024), or latent representation spaces (Cui et al., 2024; Jiang et al., 2024). Concurrently, research has focused on architectural designs to handle the heterogeneous nature of EEG electrode configurations by introducing topology-agnostic mechanisms to generalize across arbitrary electrode montages (Ouahidi et al., 2025; Fang et al., 2025), to improve scaling by exploring efficient state-models (Döner et al., 2025; Tegon et al., 2025), or to incorporate joint learning with additional modalities such as iEEG (Yuan et al., 2025), MEG (Xiao et al., 2025), and other biosignals (Luo et al., 2025). However, despite these advances in scaling and architecture, alternative pretraining objectives to masked reconstruction remain underexplored (Liu et al., 2026).

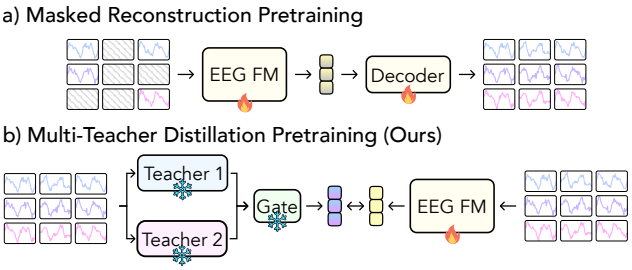

Figure 1. Comparison of EEG Foundation Model Pretraining. a) The conventional self-supervised pretraining where EEG foundation model reconstructs missing patches in the temporal, frequency or latent-domain. b) The proposed framework to bootstrap EEG foundation model pretraining by standing on the shoulders of well-established foundation models from well-represented modalities.

2.2. Repurposing Models for Time Series

The success of large-scale pretraining in natural language processing and computer vision has inspired a growing interest in repurposing or reprogramming existing FMs for time series (Li et al., 2023; Jin et al., 2024; Zhong et al., 2025), rather than training models from scratch. Early efforts investigated the feasibility of whether the structural understanding of vision transformers and the reasoning and sequential capabilities of LLMs could be transferred to time series applications. It was demonstrated that plotting irregularly sampled time series into line graph images allows pretrained vision transformers to outperform specialized baselines, offering a robust and simplified framework for extreme data scarcity (Li et al., 2023). Time-LLM (Jin et al., 2024) demonstrated that a reprogramming layer that aligns time series patches with text prototype embeddings enables LLMs to perform forecasting without changing the backbone parameters. Time-VLM (Zhong et al., 2025) further extended the repurposing paradigm to vision-language models and established a new frontier for multimodal time series forecasting. Similar cross-modal repurposing has also been

adopted for domain-specific applications, such as medical time series classification (Huang et al., 2024), zero-shot ECG learning (Li et al., 2024a), and prediction of healthcare events (Yu & Wang, 2025). These studies highlight the untapped potential of cross-modal priors for EEG representation learning, offering a promising yet unexplored path for their integration into EEG FM pretraining.

2.3. Multi-Teacher Distillation

The concept of transferring knowledge from one model to another was formalized by (Hinton et al., 2015). Although single-teacher distillation is effective, multi-teacher distillation seeks to synthesize diverse perspectives from different teacher models, through collaborative frameworks (Pham et al., 2022) or dynamic weighing of teacher contributions (Liu et al., 2020). Recent literature has increasingly explored distillation from Mixture-of-Experts (MoE) architectures (Xie et al., 2024; Al-Maamari et al., 2025; Kim et al., 2025; Li et al., 2024b). These systems can be viewed as an extension of multi-teacher frameworks, wherein a gating mechanism dynamically selects the most relevant teachers. A notable application is AM-RADIO (Ranzinger et al., 2024), which employs multi-teacher distillation to amalgamate the unique strengths of each teacher into a unified model. We adopt a similar philosophy by utilizing a learnable gate to fuse cross-modal priors, effectively treating frozen mainstream FMs as domain-specific teachers.

3. Preliminary Experiment

To evaluate the quality of representation of pretrained EEG FMs versus mainstream FMs, we perform a linear probing analysis comparing the state-of-the-art EEG FM CBraMod (Wang et al., 2025) against the vision FM DINOv3 (Siméoni et al., 2025). We extract representations from EEG signals using both models as frozen feature extractors. The cross-modal adaptation protocol used to project EEG signals into a format compatible with DINOv3 is detailed in Section 5.1.2. Finally, we evaluate the linear separability of these representations by training a logistic regression classifier that serves as a proxy for the quality of the captured neural dynamics. By restricting the classifier to a linear architecture, we ensure that the performance reflects the intrinsic quality of the representations rather than the capacity of the downstream head to compensate for poor representations.

Figure 2 compares the performance of the linear probing in a variety of downstream EEG tasks. DINOv3 consistently outperforms CBraMod across all datasets except CHB-MIT, suggesting that, compared to EEG FMs, large-scale vision FMs generalize well to EEG tasks. These findings provide strong motivation to reconsider the traditional masked reconstruction pretraining for EEG FMs, and instead explore leveraging the knowledge from mainstream FMs.

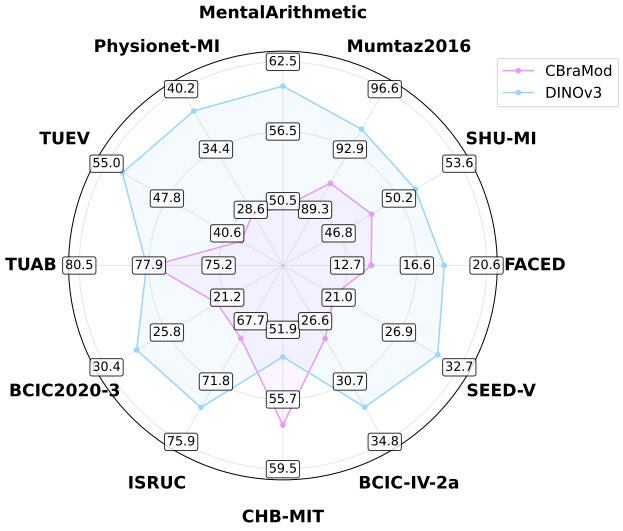

Figure 2. Linear probing performance of CBraMod and DINOv3 on EEG downstream tasks. Balanced Accuracy (%).

4. Methodology

4.1. Problem Definition

Let $\mathcal{D} = \{\mathbf{x}_i\}_{i=1}^{N}$ denote an unlabeled EEG dataset containing N samples. Each sample $\mathbf{x} \in \mathbb{R}^{C\times T}$ represents a multi-channel recording with C channels across T time steps. We define an EEG FM $f_\theta : \mathbb{R}^{C\times T} \to \mathbb{R}^d$, parameterized by θ, which serves as an encoder that maps the EEG sample $\mathbf{x}$ into a d-dimensional latent representation $\mathbf{h} \in \mathbb{R}^d$.

The objective of EEG FM pretraining is to optimize the parameters θ to maximize generalization performance across a set of N_{task} downstream tasks $\mathcal{T} = \{\mathcal{T}_t\}_{t=1}^{N_{\text{task}}}$. Each task $\mathcal{T}_t$ is associated with a dataset $\mathcal{D}_t$ partitioned into training $\mathcal{D}_t^{\text{train}}$, validation $\mathcal{D}_t^{\text{val}}$, and test $\mathcal{D}_t^{\text{test}}$ subsets. The training set consists of N_{train} EEG-label pairs, $\mathcal{D}_t^{\text{train}} = \{(\mathbf{x}_i, y_i)\}_{i=1}^{N_{\text{train}}}$, with the validation and test sets defined analogously. The pretraining optimization objective is formulated as follows:

$$\theta^* = \arg\max_{\theta} \mathbb{E}_{\mathcal{T}_t\in\mathcal{T}} \left[\mathcal{P}_t(h_{\eta_t} \circ f_{\theta_t}, \mathcal{D}_t^{\text{test}})\right] \quad (1)$$

where $\mathcal{P}_t$ denotes the performance metric (e.g., accuracy or F1-score) for the task $\mathcal{T}_t$, and h_{η_t} is a task-specific head parameterized by η_t. The operator $\circ$ denotes function composition. The adapted parameters θ_t and η_t are derived from the pretrained initialization θ and random initialization η via an adaptation algorithm $\mathbb{A}$:

$$(\theta_t, \eta_t) = \mathbb{A}(\theta, \eta, \mathcal{D}_t^{\text{train}}, \mathcal{D}_t^{\text{val}}) \quad (2)$$

The algorithm $\mathbb{A}$ typically corresponds to linear probing, where $\theta_t = \theta$, or fine-tuning. Crucially, the pretraining phase lacks prior knowledge of $\mathcal{T}$, requiring the encoder f_θ to learn universal representations of neural dynamics agnostic to tasks.

Algorithm 1 MTDP Framework: Two-Stage Multi-Teacher Distillation Pretraining

Input: Pretraining dataset $\mathcal{D}$
Pretrained teachers $\{f_{\phi_k}\}_{k=1}^{K}$
Output: EEG foundation model f_θ
▷ **Stage 1: Teacher Representation Fusion**
Initialize gating network g_ψ
Initialize prediction heads $\{p_{\xi_k}\}_{k=1}^{K}$
for iteration $\leftarrow 1$ to N_{iter} **do**
  Sample EEG $\mathbf{x} \sim \mathcal{D}$
  Apply mask $\tilde{\mathbf{x}} \leftarrow \mathbf{x} \odot \mathbf{m}$
  for $k \leftarrow 1$ to K **do**
    Compute $\tilde{\mathbf{h}}_k = f_{\phi_k}(\tilde{\mathbf{x}})$ and $\mathbf{h}_k = f_{\phi_k}(\mathbf{x})$
  end for
  Compute $\mathbf{w} = [w_1, ..., w_K] = g_\psi([\tilde{\mathbf{h}}_1; \ldots; \tilde{\mathbf{h}}_K])$
  Compute $\tilde{\mathbf{h}}_{\text{fused}} = \sum_{k=1}^{K} w_k \cdot \tilde{\mathbf{h}}_k$
  Compute $\mathcal{L}_{\text{denoise}} = \sum_{k=1}^{K} \|p_{\xi_k}(\tilde{\mathbf{h}}_{\text{fused}}) - \mathbf{h}_k\|_2^2$
  Update ψ, ξ_k using $\nabla_\psi \mathcal{L}_{\text{denoise}}, \nabla_{\xi_k} \mathcal{L}_{\text{denoise}}$
end for
▷ **Stage 2: Knowledge Distillation**
Initialize EEG foundation model f_θ
Initialize projection heads $\{q_\zeta\}_{k=1}^{K}$
for iteration $\leftarrow 1$ to N_{iter} **do**
  Sample EEG $\mathbf{x} \sim \mathcal{D}$
  Compute $\mathbf{h}_{\text{fused}} = \sum_{k=1}^{K} w_k \cdot f_{\phi_k}(\mathbf{x})$
  Compute $\mathcal{L}_{\text{distill}} = 1 - \frac{\langle q_\zeta \circ f_\theta(x), \mathbf{h}_{\text{fused}} \rangle}{||q_\zeta \circ f_\theta(x)||_2 \cdot ||\mathbf{h}_{\text{fused}}||_2}$
  Update θ, ζ using $\nabla_\theta \mathcal{L}_{\text{distill}}, \nabla_\zeta \mathcal{L}_{\text{distill}}$
end for

4.2. Two-Stage Multi-Teacher Distillation Pretraining

The core idea of the proposed MTDP framework is to pretrain EEG FMs by leveraging the knowledge from mainstream FMs. We achieve this by injecting the knowledge of well-established FMs from well-represented modalities (teachers) into an EEG FM (student) via a specialized distillation process. The choice of EEG FM architecture is flexible, which can be an existing EEG FM like CBraMod.

EEG signals are high-dimensional and non-stationary, characterized by a complex interplay of spatial, temporal, and spectral components that reflect the underlying neurophysiological activities. Although Section 3 shows that vision FMs have demonstrated promising potential to extract useful EEG representations, a single teacher often lacks the breadth to capture all of the aforementioned dimensions simultaneously. To address this, our MTDP framework seeks to synthesize complementary insights from FMs of different modalities that serve to guide the EEG model toward a holistic understanding of the multifaceted nature of EEG more effectively than any single teacher could alone.

To leverage the complementary representations from different modalities, our MTDP framework has two stages:

- **Stage 1: Teacher Representation Fusion.** We introduce a learnable gating network to weigh the importance of each teacher model using a masked latent denoising objective. The goal is to synthesize a unified teacher representation in an unsupervised manner.
- **Stage 2: Knowledge Distillation.** The unified teacher representation serves as the distillation target for a randomly initialized EEG FM student. The goal is to transfer the synthesized knowledge from different teachers into a compact EEG FM.

An overview of the method is illustrated in Figure 3.

4.2.1. Stage 1: Teacher Representation Fusion

The main challenge in the fusion of teacher representation is to identify the relative importance of each teacher in an unsupervised manner. Although teachers can be weighted using task-specific objective functions, such functions are unavailable during unsupervised pretraining when downstream tasks are unknown. To address this issue, we design a masked latent denoising objective to automatically weigh each teacher. Intuitively, the objective encourages the fusion of masked teacher representations such that it can best predict each of the unmasked teacher representations.

Given an EEG sample $\mathbf{x}$ from the pretraining dataset $\mathcal{D}$, we construct a masked version $\tilde{\mathbf{x}}$ by applying a binary mask $\mathbf{m} \in \{0, 1\}^{C \times T}$:

$$\tilde{\mathbf{x}} = \mathbf{x} \odot \mathbf{m}, \tag{3}$$

where $\odot$ denotes element-wise product. We apply two types of masking strategies:

- **Segment Masking**: A contiguous window between one to two seconds is masked across all channels to encourage the model to learn temporal dynamics.
- **Channel Dropout**: A random channel is dropped for all timesteps to capture spatial correlation and redundancy.

Let $\{f_{\phi_k}\}_{k=1}^{K}$ be a set of K pretrained teacher models, where each model is parametrized by ϕ_k. For each teacher k, we extract the representation from the unmasked and masked EEG samples:

$$\mathbf{h}_k = f_{\phi_k}(\mathbf{x}) \quad \text{and} \quad \tilde{\mathbf{h}}_k = f_{\phi_k}(\tilde{\mathbf{x}}) \tag{4}$$

Let g_ψ be the gating network parametrized by ψ. The gate takes as input the concatenated masked teacher representations and outputs a scalar weight for each teacher:

$$\mathbf{w} = [w_1, w_2, \ldots, w_K] = g_\psi([\tilde{\mathbf{h}}_1; \tilde{\mathbf{h}}_2; \ldots; \tilde{\mathbf{h}}_K]) \tag{5}$$

The fused teacher representation is computed as the weighted sum of the teacher representations:

$$\tilde{\mathbf{h}}_{\text{fused}} = \sum_{k=1}^{K} w_k \cdot \tilde{\mathbf{h}}_k \tag{6}$$

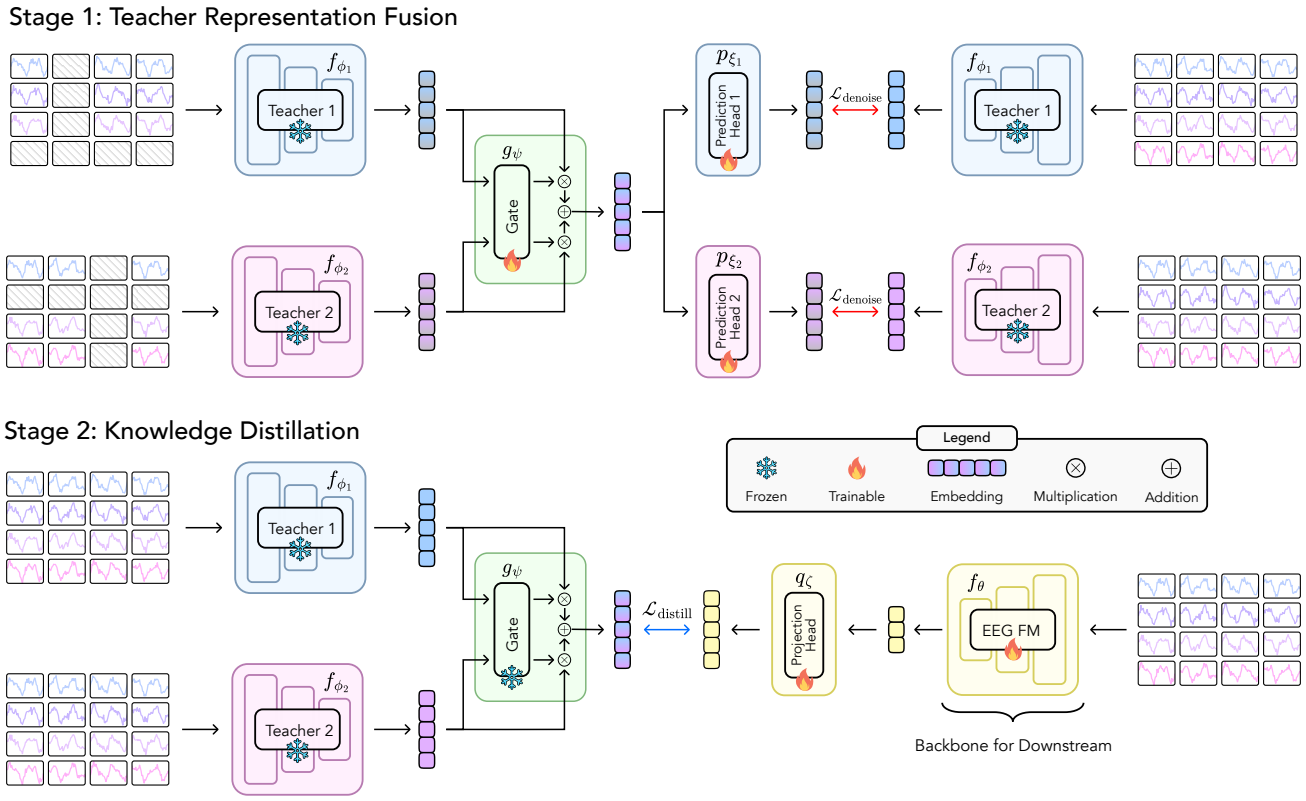

Figure 3. Overview of Two-Stage Multi-Teacher Distillation Pretraining (MTDP). Stage 1: Teacher Representation Fusion. A learnable gating network is introduced to weigh and fuse representations from frozen teacher models. The gate is trained via a masked latent denoising objective. Stage 2: Knowledge Distillation. The fused teacher representation acts as the target to pretrain the student EEG foundation model. The distillation loss is minimized to align the student representations with the fused representations.

The fused representation $\tilde{\mathbf{h}}_{\text{fused}}$ amalgamates the representations from different teachers and will serve as the distillation target for stage 2, facilitating the transfer of knowledge from multiple teachers into an EEG FM student. The gating network is trained using the masked latent denoising objective:

$$\mathcal{L}_{\text{denoise}} = \sum_{k=1}^{K} \|p_{\xi_k}(\tilde{\mathbf{h}}_{\text{fused}}) - \mathbf{h}_k\|_2^2, \tag{7}$$

where $\{p_{\xi_k}\}_{k=1}^K$ is a set of prediction heads parametrized by ξ_k for each teacher.

4.2.2. Stage 2 Knowledge Distillation

With the pretrained gating network, the objective of stage 2 is to distill the fused teacher representation into the student model. For an EEG sample $\mathbf{x}$ from the pretraining dataset, we compute the representation from each teacher $\mathbf{h}_k = f_{\phi_k}(\mathbf{x})$ and the weight for each teacher $\mathbf{w} = [w_1, \ldots, w_K] = g_\psi([\mathbf{h}_1; \mathbf{h}_2; \ldots; \mathbf{h}_K])$. The fused representation is computed as:

$$\mathbf{h}_{\text{fused}} = \sum_{k=1}^{K} w_k \cdot \mathbf{h}_k \tag{8}$$

To train the student model, we minimize the distillation loss as the cosine similarity between the student representation and the target fused teacher representation:

$$\mathcal{L}_{\text{distill}} = 1 - \frac{\langle q_\zeta \circ f_\theta(x), \mathbf{h}_{\text{fused}} \rangle}{||q_\zeta \circ f_\theta(x)||_2 \cdot ||\mathbf{h}_{\text{fused}}||_2}, \tag{9}$$

where q_ζ is a learnable projection head parameterized by ζ to match the dimensionality of the student representation with that of the fused teacher representation. $\langle \cdot, \cdot \rangle$ denotes the inner product operator. For downstream fine-tuning, teacher models $\{f_{\phi_k}\}_{k=1}^K$, gating network g_ψ, prediction heads $\{p_{\xi_k}\}_{k=1}^K$, and projection head q_ζ are discarded.

A detailed description of the MTDP Framework is provided in Algorithm 1.

5. Experiments

5.1. Experimental Setups

5.1.1. Teacher and Student Models

For the student, we adopt CBraMod (Wang et al., 2025) as the EEG FM with 4M parameters, consisting of patch encoders, positional encoder, and criss-cross transformer.

Table 1. Overview of Downstream Datasets

Task	Dataset	Rate	# Channels	Duration	# Samples	Label
Motor Imagery Classification	PhysioNet-MI	160 Hz	64	4s	9,837	4-class
	SHU-MI	250 Hz	32	4s	11,988	2-class
	BCIC-IV-2a	250 Hz	22	4s	5088	4-class
Emotion Recognition	FACED	250 Hz	32	10s	10,332	9-class
	SEED-V	1000 Hz	62	1s	115,001	5-class
Sleep Staging	ISRUC	200 Hz	6	30s	90,187	5-class
Seizure Detection	CHB-MIT	256 Hz	16	10s	326,993	2-class
Imagined Speech Classification	BCIC2020-3	256 Hz	64	3s	6,000	5-class
Mental Disorder Diagnosis	Mumtaz2016	256 Hz	19	5s	7,143	2-class
Mental Stress Detection	MentalArithmetic	500 Hz	20	5s	1,707	2-class
Event Type Classification	TUEV	250 Hz	16	5s	113,353	6-class
Abnormal Detection	TUAB	250 Hz	16	10s	409,455	2-class

The architecture is detailed in 4. For teachers, we adopt DINOv3-ViT-B/16 (Siméoni et al., 2025) and Chronos-Bolt-Base (Ansari et al., 2024). DINOv3-ViT-B/16 is distilled from DINOv3-7B that is pretrained on 1.7 billion images. It is based on the ViT-B/16 (Dosovitskiy, 2020) architecture with 87M parameters, consisting of a 12-layer transformer encoder. Chronos-Bolt-Base is a zero-shot time series forecasting model pretrained on nearly 100 billion time series observations. Chronos-Bolt-Base is based on the T5-Efficient-Base (Tay et al., 2021) architecture with 205M parameters, consisting of a 12-layer transformer encoder and 12-layer transformer decoder. We extract representations from the encoder only, as the decoder is designed for generative forecasting.

5.1.2. Preprocessing EEG for Teachers

While numerous strategies are available for preprocessing EEG signals for DINOv3 and Chronos, we adopt the Occam Razor's principle, prioritizing minimal computational overhead. DINOv3 expects images, which are represented as tensors of shape $\mathbb{R}^{3\times H\times W}$, where H and W are the height and width. EEG signals are tensors of shape $\mathbb{R}^{C\times T}$, which can be considered as single-channel images with height C and width T. We preprocesss EEG via min-max normalization to 0-1. We apply min-max normalization to scale the EEG signal to the $[0, 1]$ range, followed by a replication of the data over three channels. We also experimented with the spectrogram and continuous wavelet transform to provide additional phase-frequency information, but they introduced significant computational overhead and did not result in significant differences in performance. Chronos expects univariate time series, which are tensors of shape $\mathbb{R}^{L}$, where L is the sequence length. The EEG channels are processed independently, and the mean representation across all channels is used.

5.1.3. Pretraining and Downstream Datasets

Pretraining Dataset and Preprocessing. Following (Wang et al., 2025), we adopt the Temple University Hospital EEG Corpus (TUEG) for pretraining (Obeid & Picone, 2016), in order to ensure fair comparison between the self-supervised and the distillation pretraining strategy. Appendix Section A.1 describes the preprocessing pipeline.

Downstream Datasets. To assess the performance and generalizability of the proposed method, we conduct evaluations on 12 publicly available downstream datasets. We follow the preprocessing pipeline and subject-independent dataset splits adopted in CBraMod (Wang et al., 2025). Table 1 summarizes all the downstream datasets.

5.1.4. Training and Evaluation Details

Pretraining Stage 1 Teacher Representation Fusion. The gating network consists of a 2-layer MLP with ReLU activation between the layers and softmax activation to normalize the weights. The prediction heads consist of a single fully connected layer. Mean Squared Error (MSE) loss is adopted as the masked latent denoising objective.

Pretraining Stage 2 Knowledge Distillation. The pretrained weights for the gating network from stage 1 are loaded and frozen during stage 2 knowledge distillation. The projection head consists of a single fully connected layer. Cosine similarity is adopted as the distillation objective to minimize the distance between the projected student representations and the fused teacher representation.

Training Setup. Across both stages, we adopted a batch size of 64 per GPU across four V100 GPUs, resulting in a global batch size of 256. To avoid redundant teacher inference during distillation, teacher representations were pre-computed and stored prior to the start of the distillation process. The gate is trained for one epoch in less than an hour. Distillation on a 25% subset of the TUEG dataset over

Table 2. Comparison of EEG foundation model performance on 12 downstream tasks. "25%" and "100%" indicate pretraining dataset size compared to CBraMod. Metrics acronyms: Balanced Accuracy (B. Acc.), Weighted F1 (F1-W), Cohen's Kappa (Kappa).

Methods	Pretrain Dataset (Hours)	FACED			Physionet-MI			SHU-MI		
		B. Acc.	AUC-PR	AUROC	B. Acc.	AUC-PR	AUROC	B. Acc.	Kappa	F1-W
BIOT (Yang et al., 2023)	122	51.18	44.76	51.36	61.53	48.75	61.58	61.79	67.70	66.09
LaBraM (Jiang et al., 2024)	2500	52.73	46.98	52.88	61.73	49.12	61.77	61.66	67.61	66.04
CBraMod (Wang et al., 2025)	9000	55.09	50.41	56.18	64.17	52.22	64.27	63.70	71.39	69.88
CBraMod-MTDP 25% (Ours)	2250	56.57	50.74	56.51	62.74	50.31	62.68	**63.78**	**71.58**	**70.52**
CBraMod-MTDP 100% (Ours)	9000	**56.95**	**51.29**	**57.35**	**64.57**	**52.75**	**64.70**	62.84	71.11	69.07
Δ = *Ours* − *CBraMod*		+1.86	+0.88	+1.17	+0.40	+0.53	+0.43	-0.86	-0.28	-0.81

Methods	Pretrain Dataset (Hours)	BCIC2020-3			Mumtaz2016			MentalArithmetic		
		B. Acc.	AUC-PR	AUROC	B. Acc.	Kappa	F1-W	B. Acc.	Kappa	F1-W
BIOT (Yang et al., 2023)	122	49.20	36.50	49.17	93.58	97.36	97.58	68.75	60.04	75.36
LaBraM (Jiang et al., 2024)	2500	50.60	38.00	50.54	94.09	97.98	97.82	69.09	59.99	77.21
CBraMod (Wang et al., 2025)	9000	53.73	42.16	53.83	95.60	99.23	99.21	72.56	62.67	79.05
CBraMod-MTDP 25% (Ours)	2250	59.87	49.83	59.91	92.72	98.52	98.45	74.65	63.08	82.49
CBraMod-MTDP 100% (Ours)	9000	**62.53**	**53.17**	**62.57**	**95.85**	**99.55**	**99.55**	**77.43**	**73.30**	**87.37**
Δ = *Ours* − *CBraMod*		+8.80	+11.01	+8.74	+0.25	+0.32	+0.34	+4.87	+10.63	+8.32

Methods	Pretrain Dataset (Hours)	ISRUC			TUEV			CHB-MIT		
		B. Acc.	AUC-PR	AUROC	B. Acc.	AUC-PR	AUROC	B. Acc.	Kappa	F1-W
BIOT (Yang et al., 2023)	122	75.27	71.92	77.90	52.81	52.73	74.92	70.68	32.77	87.61
LaBraM (Jiang et al., 2024)	2500	76.33	72.31	78.10	64.09	66.37	83.12	70.75	32.87	86.79
CBraMod (Wang et al., 2025)	9000	78.65	74.42	80.11	**66.59**	67.44	83.31	73.98	36.89	88.92
CBraMod-MTDP 25% (Ours)	2250	**79.41**	**75.54**	**80.87**	66.45	70.07	84.38	**80.13**	62.27	**94.96**
CBraMod-MTDP 100% (Ours)	9000	79.38	75.12	80.49	64.88	**71.03**	**84.65**	75.42	**65.84**	94.21
Δ = *Ours* − *CBraMod*		+0.73	+0.70	+0.38	-1.71	+3.59	+1.34	+1.44	+28.95	+5.29

Methods	Pretrain Dataset (Hours)	TUAB			SEED-V			BCIC-IV-2a		
		B. Acc.	Kappa	F1-W	B. Acc.	AUC-PR	AUROC	B. Acc.	AUC-PR	AUROC
BIOT (Yang et al., 2023)	122	79.59	87.92	88.15	38.37	22.61	38.56	47.48	29.97	46.07
LaBraM (Jiang et al., 2024)	2500	81.40	89.65	90.22	39.76	23.86	39.74	48.69	31.59	47.58
CBraMod (Wang et al., 2025)	9000	**82.49**	**92.21**	**91.56**	40.91	25.69	41.01	51.38	35.18	49.84
CBraMod-MTDP 25% (Ours)	2250	79.81	88.30	87.65	41.33	27.17	42.14	59.63	46.18	58.81
CBraMod-MTDP 100% (Ours)	9000	81.02	88.98	88.06	**41.94**	**27.82**	**42.69**	**59.81**	**46.41**	**59.11**
Δ = *Ours* − *CBraMod*		-1.47	-3.23	-3.50	+1.03	+2.13	+1.68	+8.43	+11.23	+9.27

40 epochs is completed in 21 hours. The loss curves for both are illustrated in Appendix Figure 5. Hyperparameters for pretraining is detailed in Appendix Table 4. During distillation, the gating network assigns DINOv3 a weight of 0.56 and Chronos a weight of 0.43.

Downstream Fine-tuning. Following CBraMod (Wang et al., 2025), the last layer representations are flattened and passed to a classifier. The classifier consists of a 3-layer MLP with ELU activation and dropout. The model and classifier are jointly fine-tuned for each downstream dataset over 50 epochs. The best checkpoint is saved based on validation performance and evaluated on the test set.

Baselines and Metrics. We select traditional EEG models and state-of-the-art EEG FMs as baselines. Please refer to Appendix Table 6-7 for all baselines. Our main baseline for comparison is CBraMod (Wang et al., 2025), as we adopt an identical architecture and replace the self-supervised pretraining with the proposed MTDP pretraining. We report Balanced Accuracy, AUC-PR, and AUROC for binary classification and Balanced Accuracy, Cohen's Kappa, and Weighted-F1 for multi-class classification.

Table 3. Ablation of different distillation methods

Component	Set 1	Set 2	Set 3	Set 4
Chronos	✓	×	✓	✓
DINOv3	×	✓	✓	✓
Two-Stage	×	×	×	✓
FACED	51.13	54.40	56.39	**56.57**
PhysioNetMI	62.57	62.62	62.56	**62.74**
SHU-MI	62.67	62.27	62.11	**63.78**
BCI2020-3	37.73	56.93	42.80	**59.87**

5.2. Experimental Results

5.2.1. EEG Foundation Model Comparison

Experimental results on 12 downstream datasets are presented in Table 2. We present two versions of CBraMod pretrained on 25% and 100% of TUEG using the proposed MTDP framework. "CBraMod-MTDP 25%" outperforms CBraMod on 9 out of 12 downstream datasets. When scaling the pretraining dataset to 100%, we observe improved performance across all datasets, except SHU-MI and ISRUC. "CBraMod-MTDP 100%" achieves better performance than CBraMod on 10 out of 12 downstream datasets. Compared to CBraMod, significant performance gains are observed for BCIC2020-3 (8.80/11.01/8.74%), MentalArithmetic (4.87/10.63/8.32%), CHB-MIT (1.44/28.95/5.29%), and BCIC-IV-2a (8.43/11.23/9.27%). These performance gains are notable, as we adopt an identical pretraining dataset, fine-tuning algorithm, and model architecture as CBraMod. The result highlights the merit of MTDP as a promising pretraining framework for EEG FMs.

5.2.2. Teacher Representation Fusion Ablation

In Table 3, we perform ablation studies to show the effectiveness of teacher fusion from stage 1 of the pretraining presented in Section 4.2.1. All experiments are conducted with 25% pretraining dataset. We remove teacher fusion and distill with one teacher only. Set 1 distills from Chronos. Set 2 distills from DINO. Similarly to AM-RADIO (Ranzinger et al., 2024), we also distill from both teachers by summing the loss from each teacher, as denoted by set 3. Set 4 is the full MTDP framework proposed in Section 4.2.

Comparing set 1 and set 2, we observe that distilling from Chronos is better than distilling from DINOv3 on SHU-MI, but worse on FACED, PhysioNetMI and BCI2020-3. This suggests that the individual teachers provide representations that excel for different downstream tasks. In addition, we observe that set 3 performs better than set 1 and set 2 in FACED, worse performance in SHU-MI and PhysioNetMI, and between the two in BCI2020-3. This suggests that simply summing the losses from both teachers does not always yield better performance than distilling from a single teacher. Overall, set 4 achieves the best performance across the board. This highlights the effectiveness of the proposed framework in fusing teacher representations.

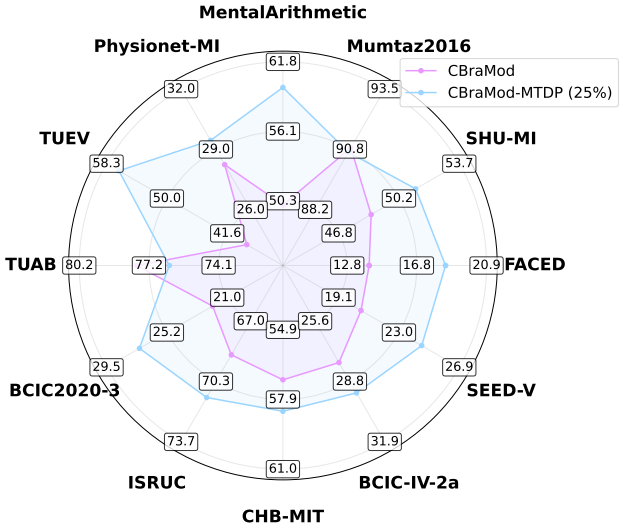

Figure 4. Linear probing performance of CBraMod and CBraMod-MTDP on EEG downstream tasks. Balanced Accuracy (%).

5.2.3. Linear Probing Comparison

Similar to Section 3, we compare the representation quality of the reconstruction-pretrained CBraMod with the distillation-pretrained CBraMod-MTDP. We extract representations from frozen CBraMod and CBraMod-MTDP 25%, then analyze the linear separability of these representations by training a logistic regression classifier. Figure 4 summarizes the linear probing performance. It is observed that CBraMod-MTDP 25% outperforms CBraMod in 10 of 12 downstream datasets. These findings suggest that the proposed framework significantly enhances the model's ability to learn generalizable representations during pretraining.

6. Conclusion

In this paper, we present a new paradigm for EEG FM pretraining by distilling from mainstream FMs. The proposed MTDP framework demonstrates consistent improvement over the masked reconstruction pretraining counterpart on the vast majority of the downstream tasks. We hope that this work inspires the community to rethink the pretraining EEG FMs and embrace the integration of cross-domain insights.

Impact Statement

This paper presents work whose goal is to advance the field of Machine Learning. There are many potential societal consequences of our work, none of which we feel must be specifically highlighted here.

References

Aboalayon, K. A. I., Faezipour, M., Almuhammadi, W. S., and Moslehpour, S. Sleep stage classification using eeg signal analysis: a comprehensive survey and new investigation. *Entropy*, 18(9):272, 2016.

Al-Maamari, M., Ben Amor, M., Mitrović, J., and Granitzer, M. Mixture of Modular Experts: Distilling Knowledge from a Multilingual Teacher into Specialized Modular Language Models. In *Proceedings of the 40th ACM/SIGAPP Symposium on Applied Computing*, pp. 945–852. 2025.

Alotaiby, T. N., Alshebeili, S. A., Alshawi, T., Ahmad, I., and Abd El-Samie, F. E. Eeg seizure detection and prediction algorithms: a survey. *EURASIP Journal on Advances in Signal Processing*, 2014(1):183, 2014.

Altaheri, H., Muhammad, G., Alsulaiman, M., Amin, S. U., Altuwaijri, G. A., Abdul, W., Bencherif, M. A., and Faisal, M. Deep learning techniques for classification of electroencephalogram (eeg) motor imagery (mi) signals: A review. *Neural Computing and Applications*, 35(20): 14681–14722, 2023.

Ansari, A. F., Stella, L., Turkmen, C., Zhang, X., Mercado, P., Shen, H., Shchur, O., Rangapuram, S. S., Arango, S. P., Kapoor, S., et al. Chronos: Learning the language of time series. *arXiv preprint arXiv:2403.07815*, 2024.

Berry, R. B., Brooks, R., Gamaldo, C., Harding, S. M., Lloyd, R. M., Quan, S. F., Troester, M. T., and Vaughn, B. V. Aasm scoring manual updates for 2017 (version 2.4), 2017.

Chen, Y., Ren, K., Song, K., Wang, Y., Wang, Y., Li, D., and Qiu, L. EEGFormer: Towards Transferable and Interpretable Large-Scale EEG Foundation Model, 2024.

Cui, W., Jeong, W., Thölke, P., Medani, T., Jerbi, K., Joshi, A. A., and Leahy, R. M. Neuro-GPT: Towards A Foundation Model for EEG, 2024.

Döner, B., Ingolfsson, T. M., Benini, L., and Li, Y. LUNA: Efficient and Topology-Agnostic Foundation Model for EEG Signal Analysis, 2025.

Dosovitskiy, A. An image is worth 16x16 words: Transformers for image recognition at scale. *arXiv preprint arXiv:2010.11929*, 2020.

Fang, Z., Li, C., Zhou, H., Yu, S., Du, G., Qasem, A., Lu, Y., Li, J., Zhang, J., and Goh, S. K. NeurIPT: Foundation Model for Neural Interfaces, 2025.

Fisher, R. S., Cross, J. H., French, J. A., Higurashi, N., Hirsch, E., Jansen, F. E., Lagae, L., Moshé, S. L., Peltola, J., Roulet Perez, E., et al. Operational classification of seizure types by the international league against epilepsy: Position paper of the ilae commission for classification and terminology. *Epilepsia*, 58(4):522–530, 2017.

Grattafiori, A., Dubey, A., Jauhri, A., Pandey, A., Kadian, A., Al-Dahle, A., Letman, A., Mathur, A., Schelten, A., Vaughan, A., et al. The llama 3 herd of models. *arXiv preprint arXiv:2407.21783*, 2024.

Hinton, G., Vinyals, O., and Dean, J. Distilling the Knowledge in a Neural Network, 2015.

Huang, N., Wang, H., He, Z., Zitnik, M., and Zhang, X. Repurposing Foundation Model for Generalizable Medical Time Series Classification, 2024.

Jiang, W.-B., Zhao, L.-M., and Lu, B.-L. Large Brain Model for Learning Generic Representations with Tremendous EEG Data in BCI, 2024.

Jin, M., Wang, S., Ma, L., Chu, Z., Zhang, J. Y., Shi, X., Chen, P.-Y., Liang, Y., Li, Y.-F., Pan, S., and Wen, Q. Time-LLM: Time Series Forecasting by Reprogramming Large Language Models, 2024.

Jing, J., Ge, W., Hong, S., Fernandes, M. B., Lin, Z., Yang, C., An, S., Struck, A. F., Herlopian, A., Karakis, I., et al. Development of expert-level classification of seizures and rhythmic and periodic patterns during eeg interpretation. *Neurology*, 100(17):e1750–e1762, 2023.

Kim, G., Chu, G., and Yang, E. Every Expert Matters: Towards Effective Knowledge Distillation for Mixture-of-Experts Language Models, 2025.

Lawhern, V. J., Solon, A. J., Waytowich, N. R., Gordon, S. M., Hung, C. P., and Lance, B. J. Eegnet: a compact convolutional neural network for eeg-based brain–computer interfaces. *Journal of neural engineering*, 15 (5):056013, 2018.

Li, H., Ding, M., Zhang, R., and Xiu, C. Motor imagery eeg classification algorithm based on cnn-lstm feature fusion network. *Biomedical signal processing and control*, 72: 103342, 2022a.

Li, J., Liu, C., Cheng, S., Arcucci, R., and Hong, S. Frozen Language Model Helps ECG Zero-Shot Learning. In *Medical Imaging with Deep Learning*, pp. 402–415, 2024a.

Li, L., Zang, H., Wang, Y., Dong, Y., and Yang, L. Multi-expert collaboration: Enhancing heterogeneous knowledge independence and alignment in knowledge distillation. 2024b.

Li, X., Zhang, Y., Tiwari, P., Song, D., Hu, B., Yang, M., Zhao, Z., Kumar, N., and Marttinen, P. Eeg based emotion recognition: A tutorial and review. *ACM Computing Surveys*, 55(4):1–57, 2022b.

Li, Z., Li, S., and Yan, X. Time Series as Images: Vision Transformer for Irregularly Sampled Time Series, 2023.

Liu, D., Chen, Y., Chen, Z., Cui, Z., Wen, Y., An, J., Luo, J., and Wu, D. Eeg foundation models: Progresses, benchmarking, and open problems, 2026. URL https://arxiv.org/abs/2601.17883.

Liu, Y., Zhang, W., and Wang, J. Adaptive Multi-Teacher Multi-level Knowledge Distillation. *Neurocomputing*, 415:106–113, 2020. doi: 10.1016/j.neucom.2020.07.048.

Luo, Y., Chen, Y., Salekin, A., and Rahman, T. Toward Foundation Model for Multivariate Wearable Sensing of Physiological Signals, 2025.

Obeid, I. and Picone, J. The temple university hospital eeg data corpus. *Frontiers in neuroscience*, 10:196, 2016.

Ouahidi, Y. E., Lys, J., Thölke, P., Farrugia, N., Pasdeloup, B., Gripon, V., Jerbi, K., and Lioi, G. REVE: A Foundation Model for EEG – Adapting to Any Setup with Large-Scale Pretraining on 25,000 Subjects, 2025.

Peh, W. Y., Yao, Y., and Dauwels, J. Transformer convolutional neural networks for automated artifact detection in scalp eeg. In *2022 44th Annual International Conference of the IEEE Engineering in Medicine & Biology Society (EMBC)*, pp. 3599–3602. IEEE, 2022.

Pham, C., Hoang, T., and Do, T.-T. Collaborative Multi-Teacher Knowledge Distillation for Learning Low Bit-width Deep Neural Networks, 2022.

Ranzinger, M., Heinrich, G., Kautz, J., and Molchanov, P. Am-radio: Agglomerative vision foundation model reduce all domains into one. In *Proceedings of the IEEE/CVF conference on computer vision and pattern recognition*, pp. 12490–12500, 2024.

Siméoni, O., Vo, H. V., Seitzer, M., Baldassarre, F., Oquab, M., Jose, C., Khalidov, V., Szafraniec, M., Yi, S., Ramamonjisoa, M., Massa, F., Haziza, D., Wehrstedt, L., Wang, J., Darcet, T., Moutakanni, T., Sentana, L., Roberts, C., Vedaldi, A., Tolan, J., Brandt, J., Couprie, C., Mairal, J., Jégou, H., Labatut, P., and Bojanowski, P. DINOv3, 2025.

Siuly, S., Li, Y., and Zhang, Y. Electroencephalogram (eeg) and its background. In *EEG signal analysis and classification: Techniques and applications*, pp. 3–21. Springer, 2017.

Song, Y., Jia, X., Yang, L., and Xie, L. Transformer-based spatial-temporal feature learning for eeg decoding. *arXiv preprint arXiv:2106.11170*, 2021.

Song, Y., Zheng, Q., Liu, B., and Gao, X. Eeg conformer: Convolutional transformer for eeg decoding and visualization. *IEEE Transactions on Neural Systems and Rehabilitation Engineering*, 31:710–719, 2022.

Tay, Y., Dehghani, M., Rao, J., Fedus, W., Abnar, S., Chung, H. W., Narang, S., Yogatama, D., Vaswani, A., and Metzler, D. Scale efficiently: Insights from pre-training and fine-tuning transformers. *arXiv preprint arXiv:2109.10686*, 2021.

Tegon, A., Ingolfsson, T. M., Wang, X., Benini, L., and Li, Y. FEMBA: Efficient and Scalable EEG Analysis with a Bidirectional Mamba Foundation Model, 2025.

Wang, J., Zhao, S., Luo, Z., Zhou, Y., Jiang, H., Li, S., Li, T., and Pan, G. CBraMod: A Criss-Cross Brain Foundation Model for EEG Decoding, 2025.

Xiao, Q., Cui, Z., Zhang, C., Chen, S., Wu, W., Thwaites, A., Woolgar, A., Zhou, B., and Zhang, C. BrainOmni: A Brain Foundation Model for Unified EEG and MEG Signals, 2025.

Xie, Z., Zhang, Y., Zhuang, C., Shi, Q., Liu, Z., Gu, J., and Zhang, G. MoDE: A Mixture-of-Experts Model with Mutual Distillation among the Experts, 2024.

Yang, C., Xiao, D., Westover, M. B., and Sun, J. Self-supervised eeg representation learning for automatic sleep staging. *arXiv preprint arXiv:2110.15278*, 2021.

Yang, C., Westover, M., and Sun, J. BIOT: Biosignal Transformer for Cross-data Learning in the Wild. *Advances in Neural Information Processing Systems*, 36:78240–78260, 2023.

Yu, T. and Wang, G. Healthcare Event Prediction via Iterative in-Context Learning of LLM. In *2025 10th International Conference on Cloud Computing and Big Data Analytics (ICCCBDA)*, pp. 205–210, 2025. doi: 10.1109/ICCCBDA64898.2025.11030505.

Yuan, Z., Zhang, D., Chen, J., Gu, G., and Yang, Y. Brant-2: Foundation Model for Brain Signals, 2024.

Yuan, Z., Shen, F., Li, M., Yu, Y., Tan, C., and Yang, Y. BrainWave: A Brain Signal Foundation Model for Clinical Applications, 2025.

Zhang, D., Yuan, Z., Yang, Y., Chen, J., Wang, J., and Li, Y. Brant: Foundation Model for Intracranial Neural Signal. In *Thirty-Seventh Conference on Neural Information Processing Systems*, 2023.

Zhong, S., Ruan, W., Jin, M., Li, H., Wen, Q., and Liang, Y. Time-VLM: Exploring Multimodal Vision-Language Models for Augmented Time Series Forecasting, 2025.

A. Experiment Setting

A.1. Pretraining Dataset Preprocessing

We select 16 channels (Fp1, Fp2, F7, F3, F4, F8, T3, C3, C4, T4, T5, P3, P4, T6, O1, O2), apply band-pass (0.3-75 Hz) and notch (60 Hz) filter, resample to 200 Hz, segment into 30-second non-overlapping segments, discard samples with absolute amplitude exceeding 100 μV, and normalize to -1 to 1 range by setting unit to 100 μV. Unlike CBraMod, we apply an additional step to remove TUAB and TUEV samples to avoid downstream data contamination. This results in a total of 1,059,523 samples, which is around 8,829 hours in total.

A.2. Pretraining Hyperparameters

Table 4 summarizes the hyperparameters used for pretraining.

Table 4. Pretraining Hyperparameters

Hyperparameters	Settings
Data	
Channels	16
Time points	6000
Patch dimension	200
Sequence length	30 s
CBraMod Model Architecture	
Patch Encoder (Time-Domain)	
Input dimension	{1, 25, 25}
Output dimension	{25, 25, 25}
Kernel size	{49, 3, 3}
Stride	{25, 1, 1}
Padding	{24, 1, 1}
Patch Encoder (Freq-Domain)	
FFT function	torch.fft.rfft
Fully-connected layer	(101, 200)
Positional Encoder	
Input dimension	200
Output dimension	200
Kernel size	(19, 7)
Stride	(1, 1)
Padding	(9, 3)
Criss-cross Transformer	
Layers	12
Hidden dimension	200
Heads	8
S-Attention heads	4
T-Attention heads	4
Feed-forward dimension	800

Hyperparameters	Settings
Stage 1 Teacher Representation Fusion	
Epochs	1
Batch size	256
Optimizer	AdamW
Learning rate	5e-4
Adam β	(0.9, 0.999)
Adam ϵ	1e-8
Weight decay	5e-2
Clipping gradient norm	1
Weights init	Kaiming normalization
Loss	MSELoss
Stage 2 Knowledge Distillation	
Epochs	40
Batch size	256
Optimizer	AdamW
Learning rate	5e-4
Adam β	(0.9, 0.999)
Adam ϵ	1e-8
Weight decay	5e-2
Scheduler	CosineAnnealingLR
Cosine cycle epochs	40
Minimal learning rate	1e-5
Clipping gradient norm	1
Weights init	Kaiming normalization
Loss	CosineEmbeddingLoss

A.2.1. Training Loss Curves

Figure 5 plots the loss curve of stage 1 and stage 2 pretraining.

A.3. Fine-tuning Hyperparameters

We adopt the fine-tuning code from CBraMod without any modification. We load our distilled checkpoint instead of the self-supervised checkpoint provided by CBraMod. Following CBraMod, we perform a grid search over three different learning rates and a binary multi-LR setting. Multi-LR adjusts the classifier learning rate to be five times larger. Table 5 summarizes the fine-tuning hyperparameters.

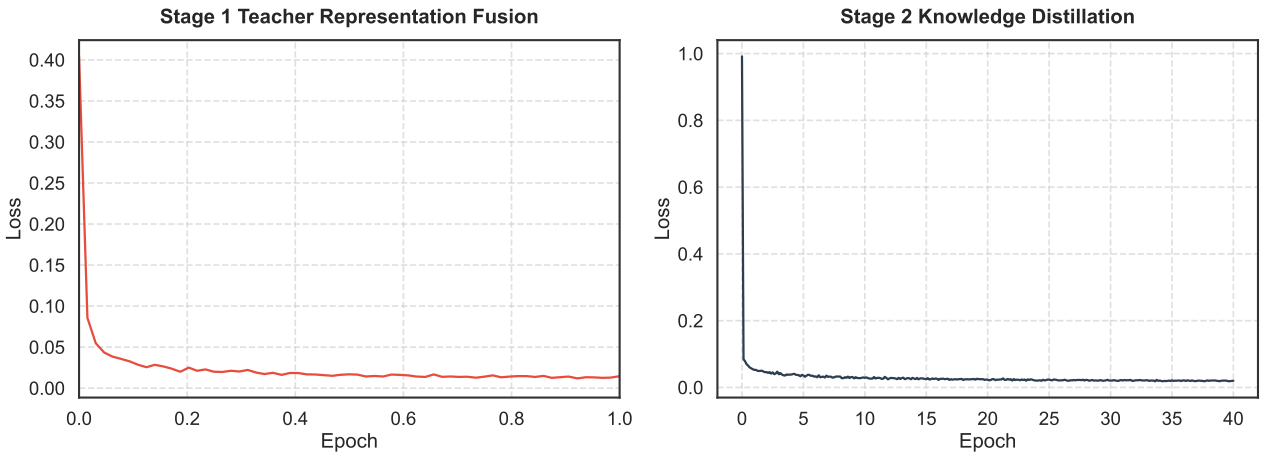

Figure 5. Loss curve of stage 1 and stage 2 pretraining

Table 5. Fine-tuning Hyperparameters

Hyperparameters	**Settings**
Epochs	50
Batch size	64
Dropout	0.1
Optimizer	AdamW
Bakbone Learning rate	{5e-5, 1e-4, 5e-4}
Multi-LR	{Yes, No}
Adam β	(0.9, 0.999)
Adam ϵ	1e-8
Weight decay	5e-2
Scheduler	CosineAnnealingLR
Cosine cycle epochs	50
Minimal learning rate	1e-6
Clipping gradient norm	1
Label smoothing (multi-class classification)	0.1

B. Comparison with Traditional EEG Models and EEG Foundation Models

We compare against traditional EEG models and EEG FMs. The traditional models include: EEGNet (Lawhern et al., 2018), EEGConformer (Song et al., 2022), SPaRCNet (Jing et al., 2023), ContraWR (Yang et al., 2021), CNN-Transformer (Peh et al., 2022), FFCL (Li et al., 2022a), ST-Transformer (Song et al., 2021). The EEG FMs include BIOT (Yang et al., 2023) and LaBraM (Jiang et al., 2024). Table 6-7 presents the full results.

Table 6. Comparison of EEG foundation model performance on 12 downstream tasks (Part 1/2). "25%" and "100%" indicate pretraining dataset size compared to CBraMod. Metrics acronyms: Balanced Accuracy (B. Acc.), Weighted F1 (F1-W), Cohen's Kappa (Kappa).

Methods	Pretrain Dataset (Hours)	FACED			Physionet-MI			SHU-MI		
		B. Acc.	AUC-PR	AUROC	B. Acc.	AUC-PR	AUROC	B. Acc.	Kappa	F1-W
EEGNet	0	40.90	33.42	41.24	58.14	44.68	57.96	58.89	63.11	62.83
EEGConformer	0	45.59	38.58	45.14	60.49	47.36	60.62	59.00	63.70	63.51
SPaRCNet	0	46.73	39.78	47.29	59.32	45.64	59.37	59.78	65.10	64.31
ContraWR	0	48.87	42.31	48.84	58.92	45.27	59.18	58.73	63.15	62.73
CNN-Transformer	0	46.97	40.17	47.20	60.53	47.25	60.41	59.75	64.12	63.23
FFCL	0	46.73	39.87	46.99	57.26	43.23	57.01	56.92	59.43	60.14
ST-Transformer	0	48.10	41.37	47.95	60.35	47.12	60.53	59.92	63.94	64.31
BIOT	122	51.18	44.76	51.36	61.53	48.75	61.58	61.79	67.70	66.09
LaBraM	2500	52.73	46.98	52.88	61.73	49.12	61.77	61.66	67.61	66.04
CBraMod	9000	55.09	50.41	56.18	64.17	52.22	64.27	63.70	71.39	69.88
CBraMod-MTDP 25% (Ours)	2250	56.57	50.74	56.51	62.74	50.31	62.68	**63.78**	**71.58**	**70.52**
CBraMod-MTDP 100% (Ours)	9000	**56.95**	**51.29**	**57.35**	**64.57**	**52.75**	**64.70**	62.84	71.11	69.07
$\Delta = Ours - CBraMod$		+1.86	+0.88	+1.17	+0.40	+0.53	+0.43	-0.86	-0.28	-0.81

Methods	Pretrain Dataset (Hours)	BCIC2020-3			Mumtaz2016			MentalArithmetic		
		B. Acc.	AUC-PR	AUROC	B. Acc.	Kappa	F1-W	B. Acc.	Kappa	F1-W
EEGNet	0	44.13	30.16	44.13	92.32	96.26	96.39	67.70	57.63	73.21
EEGConformer	0	45.06	31.33	44.88	93.08	96.84	97.02	68.05	58.29	74.24
SPaRCNet	0	44.26	30.33	44.20	93.16	97.54	97.81	68.79	58.25	74.18
ContraWR	0	42.57	30.78	44.07	91.95	95.89	96.21	66.31	57.87	73.32
CNN-Transformer	0	45.33	31.66	45.06	93.05	97.57	97.42	67.79	57.77	72.58
FFCL	0	46.78	33.01	46.89	93.14	97.17	97.53	67.98	57.86	73.30
ST-Transformer	0	41.26	29.41	42.47	91.35	95.78	95.94	66.31	56.72	71.32
BIOT	122	49.20	36.50	49.17	93.58	97.36	97.58	68.75	60.04	75.36
LaBraM	2500	50.60	38.00	50.54	94.09	97.98	97.82	69.09	59.99	77.21
CBraMod	9000	53.73	42.16	53.83	95.60	99.23	99.21	72.56	62.67	79.05
CBraMod-MTDP 25% (Ours)	2250	59.87	49.83	59.91	92.72	98.52	98.45	74.65	63.08	82.49
CBraMod-MTDP 100% (Ours)	9000	**62.53**	**53.17**	**62.57**	**95.85**	**99.55**	**99.55**	**77.43**	**73.30**	**87.37**
$\Delta = Ours - CBraMod$		+8.80	+11.01	+8.74	+0.25	+0.32	+0.34	+4.87	+10.63	+8.32

Table 7. Comparison of EEG foundation model performance on 12 downstream tasks (Part 2/2). "25%" and "100%" indicate pretraining dataset size compared to CBraMod. Metrics acronyms: Balanced Accuracy (B. Acc.), Weighted F1 (F1-W), Cohen's Kappa (Kappa).

Methods	Pretrain Dataset (Hours)	ISRUC			TUEV			CHB-MIT		
		B. Acc.	AUC-PR	AUROC	B. Acc.	AUC-PR	AUROC	B. Acc.	Kappa	F1-W
EEGNet	0	71.54	70.40	75.13	38.76	35.77	65.39	56.58	19.14	80.48
EEGConformer	0	74.00	71.43	76.34	40.74	39.67	69.83	59.76	22.09	82.26
SPaRCNet	0	74.87	70.97	76.24	41.61	42.33	70.24	58.76	12.47	81.43
ContraWR	0	74.02	71.78	76.10	43.84	39.12	68.93	63.44	22.64	80.97
CNN-Transformer	0	73.63	71.29	77.19	40.87	38.15	68.54	63.89	24.79	86.62
FFCL	0	72.77	70.16	76.14	39.79	37.32	67.83	62.62	20.49	82.71
ST-Transformer	0	73.81	70.13	76.81	39.84	37.65	68.23	59.15	14.22	82.37
BIOT	122	75.27	71.92	77.90	52.81	52.73	74.92	70.68	32.77	87.61
LaBraM	2500	76.33	72.31	78.10	64.09	66.37	83.12	70.75	32.87	86.79
CBraMod	9000	78.65	74.42	80.11	**66.59**	67.44	83.31	73.98	36.89	88.92
CBraMod-MTDP 25% (Ours)	2250	**79.41**	**75.54**	**80.87**	66.45	70.07	84.38	**80.13**	62.27	**94.96**
CBraMod-MTDP 100% (Ours)	9000	79.38	75.12	80.49	64.88	**71.03**	**84.65**	75.42	**65.84**	94.21
$\Delta = Ours - CBraMod$		+0.73	+0.70	+0.38	-1.71	+3.59	+1.34	+1.44	+28.95	+5.29

Methods	Pretrain Dataset (Hours)	TUAB			SEED-V			BCIC-IV-2a		
		B. Acc.	Kappa	F1-W	B. Acc.	AUC-PR	AUROC	B. Acc.	AUC-PR	AUROC
EEGNet	0	76.42	82.99	84.12	29.61	10.06	27.49	44.82	26.93	42.26
EEGConformer	0	77.58	84.27	84.45	35.37	17.72	34.87	46.96	29.24	45.33
SPaRCNet	0	78.96	84.14	86.76	29.49	11.21	29.79	46.35	28.47	44.32
ContraWR	0	77.46	84.21	84.56	35.46	19.05	35.44	46.78	29.05	44.13
CNN-Transformer	0	77.77	84.33	84.61	36.78	20.72	36.42	46.00	28.00	44.60
FFCL	0	78.48	84.48	85.69	36.41	20.78	36.45	44.70	26.27	42.38
ST-Transformer	0	79.66	85.21	87.07	30.52	10.83	28.33	45.75	27.33	44.71
BIOT	122	79.59	87.92	88.15	38.37	22.61	38.56	47.48	29.97	46.07
LaBraM	2500	81.40	89.65	90.22	39.76	23.86	39.74	48.69	31.59	47.58
CBraMod	9000	**82.49**	**92.21**	**91.56**	40.91	25.69	41.01	51.38	35.18	49.84
CBraMod-MTDP 25% (Ours)	2250	79.81	88.30	87.65	41.33	27.17	42.14	59.63	46.18	58.81
CBraMod-MTDP 100% (Ours)	9000	81.02	88.98	88.06	**41.94**	**27.82**	**42.69**	**59.81**	**46.41**	**59.11**
$\Delta = Ours - CBraMod$		-1.47	-3.23	-3.50	+1.03	+2.13	+1.68	+8.43	+11.23	+9.27

C. Limitations

The use of DINOv3 and Chronos incurs additional data processing and inference cost, compared to masked reconstruction pretraining. Although we minimize this cost by storing the teacher representations, it introduces additional hard disk and I/O burdens.